Novel Multi-Aperture 3D Imaging Systems

J.C. Marron, R. L. Kendrick*, T. A. Höft, and N. Seldomridge

Lockheed Martin Coherent Technologies
135 South Taylor Ave.
Louisville, CO 80027
joe.marron@lmco.com

*R.L. Kendrick is with Lockheed Martin Advanced Technology Center, Palo Alto, CA.

INTRODUCTION

With a multi-aperture, active imaging system, one creates a large imaging aperture by digitally combining the light from a series of distributed telescopes [1]. In doing this, one can construct a fine-resolution imaging system with reduced volume. Furthermore, by incorporating a wavelength tunable laser source, one can recover 3D images. In such a system, the image formation process incorporates digital correction of optical and atmospheric phase errors. Here we discuss the principles underlying this method and present results from laboratory experiments.

A schematic for a distributed aperture, coherent imaging system is shown in Figure 1. Here the object is flood-illuminated with laser light from a coherent source. The scattered light is then collected by a series of smaller telescopes, each having a coherent detection system that records the amplitude and phase of the light over the entrance pupil. This process requires coherent detection with an array detector. Below we discuss the detection process in greater detail.

figu

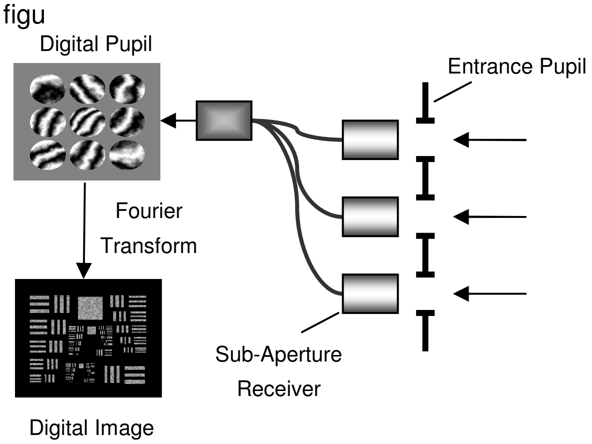

Figure. 1. Distributed aperture coherent imaging system. Data from the entrance pupil is recorded digitally by each of the sub-apertures and re-assembled into larger numerical array corresponding to the entire entrance pupil. The image is then formed by digital Fourier transformation.

The result of coherent detection in the sub-apertures is a series of arrays of digital, complex-valued numbers that correspond to the optical field measured over the receiver sub-aperture. These digital numbers are then combined into a digital replica of the entire entrance pupil. As with a passive system, this digital replica is a precise version of the entrance pupil. For example, data from the individual sub apertures must be positioned properly, with the correct magnification and rotation. If the mapping is not precise, phase errors occur that result in image aberrations, including field dependent aberrations.

An important feature of a distributed aperture coherent imaging system is that the pupil re-imaging system required for an incoherent distributed aperture system is eliminated. Furthermore, the pupil mapping, and aberrations imparted by imperfect pupil mapping, can be controlled digitally, as opposed to the optical correction required in an incoherent distributed aperture system. Finally, the distributed aperture coherent imaging system can allow for digital correction of aberrations imparted by atmospheric turbulence.

The procedure that we use for aperture alignment and correction of atmospherically induced phase errors is based on maximizing an image sharpness criterion [2]. With this procedure, one begins with the aberrated pupil, and aberrated image, and applies phase errors, or pupil mapping corrections, in a systematic manner to maximize image quality as measured by the sharpness metric. Researchers have developed efficient algorithms for determining the phase aberrations for a variety of objects and noise conditions [3]. Figure 2 contains an illustration of this process. Note that this process is digital and thus can operate at high-

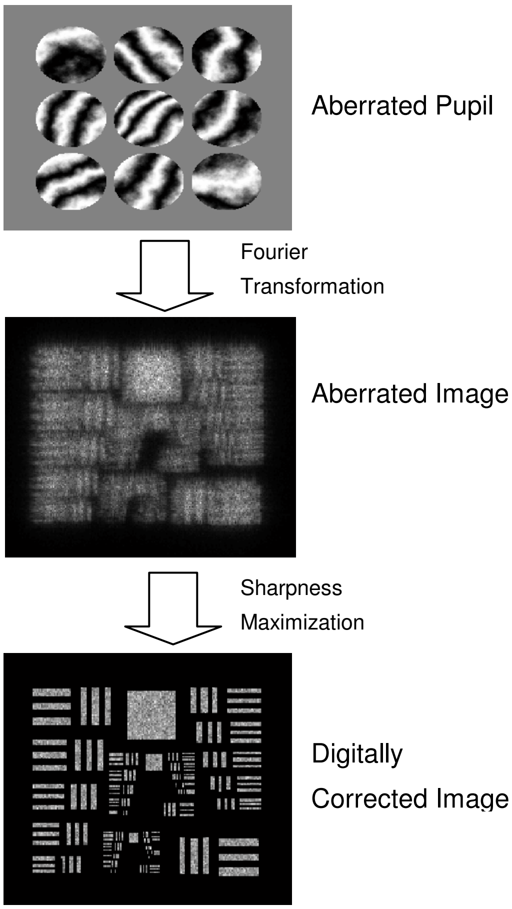

Figure 2. Illustration of digital method for aberration determination

rates in contrast to slower speed operation that can result with an actuated system involving mechanical components as required for incoherent versions.

In order to accomplish distributed aperture coherent imaging, we require a method for coherently detecting the optical field over a segment of the entrance pupil. The method that we use is often referred to as spatial heterodyne detection. This method is basically a variation of optical holography with digital recording [4].

With spatial heterodyne detection, the distant object is flood illuminated with coherent light and the return light is imaged through the sub-aperture onto a field stop. After the field stop, a beamsplitter introduces a reference point or local oscillator. This reference point then interferes with the light from the object and the interference pattern is recorded by a 2D detector array. Note that the detector output is essentially a speckle pattern with a superimposed fringe pattern with spatial frequency corresponding to the angular separation of the reference point and the field stop. An example speckle pattern is shown in Fig. 3.

The coherent field data in the pupil plane is derived from the detector output by a simple Fourier transform illustrated in Fig. 4. This figure shows that the complex valued image is obtained by simply extracting a section of the digital Fourier transform of, for example, the intensity pattern in Fig. 3.

We have conducted a series of laboratory experiments that demonstrate distributed aperture active imaging with a 4 aperture system. This system is comprised of 4 receiver apertures that sense a target imaged to infinity by a collimator. light from the target is received by the individual sub apertures. In the subapertures, the received light is interfered with coherent light from the local oscillator. Coherent data from the individual sub-apertures is then assembled into a larger data array. An example data array corresponding to the 4 apertures is shown in Fig. 5. The individual sub apertures are partially obscured by circular secondaries. An additional obscuration arises from the secondary of the collimating telescope.

An example image corresponding to all 4 apertures is shown in the lower portion of Fig. 5. Eight speckle realizations were averaged to obtain this image. These results demonstrate the ability to form

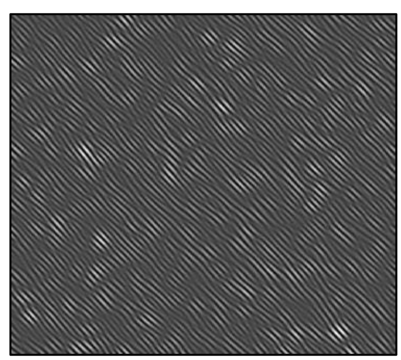

Figure 3. Example of detector array output from spatial heterodyne detection. Note the spatial carrier frequency.

diffraction limited images by compensating individual apertures for instrumentation errors and laboratory turbulence.

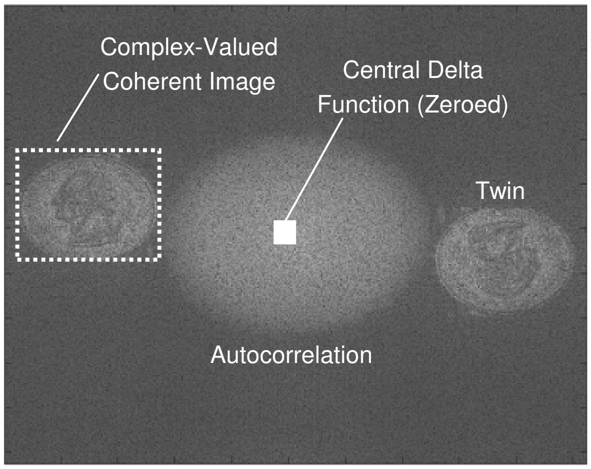

Fig. 5. Complex-valued coherent image is obtained by extracting a segment of the Fourier transform of the detected intensity data. This result is from laboratory data with the object being a coin.

3D IMAGING

One can also perform 3D imaging by incorporating a tunable source into the imaging systems described above [5]. To demonstrate this we conducted a series of experiments using a single aperture system. The coherent images used in these experiments were recorded using spatial heterodyne detection as described above. Again, light from a tunable laser source is split into two components: an object beam and a reference beam. The object beam illuminates the diffuse object and the backscattered light is incident on the detector array. This light is interfered coherently with the reference beam and complex-valued data is then derived from the interference pattern recorded by the detector array.

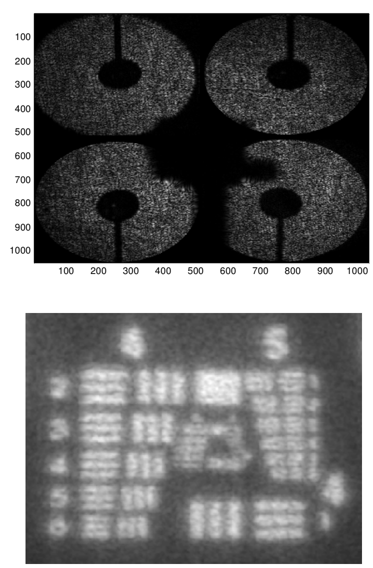

Fig. 7. Experimental results from the instrumentation shown in Figure 6. An example of the digitally formed pupil is shown on the left with a corresponding image shown on the right. The image on the right results from an average of 8 speckle realizations.

Before computing the 3D image, aberrations were removed from the component images. While the primary aberration was defocus, other higher-order aberrations were also removed. To accomplish this we maximized image sharpness. Coherent images before and after focusing are shown in Figure 6. Notice that before focusing, features of the image are not recognizable. Also note that convergence of the focusing algorithm and image appearance are enhanced by using multiple speckle realizations.

With the complex-valued data recorded at the two wavelengths, 3D images are found by taking the phase difference of the two images on a pixel-by-pixel basis. Note that distance determination with this method is subject to ambiguity interval limitation with the ambiguity interval given by $c/2(\nu_1-\nu_2)$.

Image results of data collected using this two-wavelength method is shown below. Fig. 7 contains the reflectivity image of a scale model truck and Fig. 8 shows the corresponding gray-scale encoded 3D image. These images resulted from averaging 8 pairs of two-wavelength data.

For these experiments the frequency separation of the laser wavelengths was set so that the imaging ambiguity interval was greater than the depth of the object. By doing this we avoided the need for unwrapping the image.

CONCLUSION

In this paper we have discussed novel imaging concepts involving multi-aperture laser radar systems that perform fine resolution 3D imaging. The image formation process for these methods is digital and uses coherent image data from a series of modular sub apertures. In doing this, aberrations from the atmosphere and optical misalignment can corrected via digital processing and thus avoid the need for complicated optical beam combining.

The detection process used is often called spatial heterodyne detection; it allows complex valued image detection via straightforward Fourier transform processing.

Additionally we have demonstrated that the methods are capable of 3D imaging by constructing 3D images from two-wavelength laboratory data.

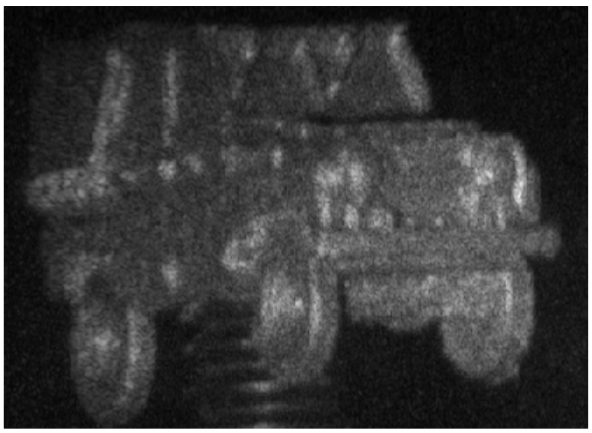

Fig. 3. Intensity image produced from two-wavelength LADAR data. Eight speckle realizations were used.

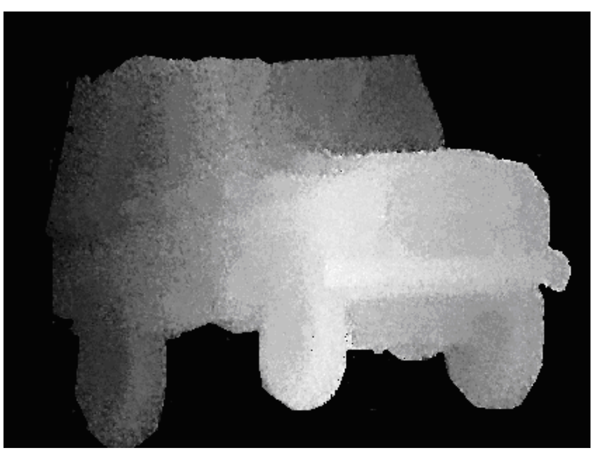

Fig. 4. Three dimensional image produced from two-wavelength LADAR. Range is encoded as gray-scale. Eight speckle realizations were used to form this image.

REFERENCES

[1] J.C. Marron, R.L. Kendrick, "Distributed Aperture Active Imaging," Proc SPIE 6550-11, (2007).

[2] R.G. Paxman and J.C. Marron. "Aberration Correction of Speckled Imagery With an Image Sharpness Criterion," Proc. SPIE Conference on Statistical Optics, 976, San Diego, CA, August 1988.

[3] J. R. Fienup and J. J. Miller, "Aberration correction by maximizing generalized sharpness metrics," J. Opt. Soc. Am. A, 20, 609-620 (April 2003)

[4] J.C. Marron and K.S. Schroeder, "Holographic Laser Radar," Opt. Lett., 18, 385-387, 1993.

[5] J. C. Marron and K. W. Gleichman, "Three-Dimensional Imaging Using a Tunable Laser Source," Optical Engineering, 39, 47-51, 2000.